

Single Component Molecular Resists Containing Bound Photoacid Generator Functionality

Richard A. Lawson^a, Laren M. Tolbert^b, Clifford L. Henderson^{a*}

^aSchool of Chemical & Biomolecular Engineering, Georgia Institute of Technology
Atlanta, GA 30332-0100

^bSchool of Chemistry and Biochemistry, Georgia Institute of Technology
Atlanta, GA 30332

* Corresponding Author: cliff.henderson@chbe.gatech.edu

ABSTRACT

A series of single component molecular resists were designed, synthesized, characterized, and patterned using 100 keV e-beam lithography. An onium salt PAG based single component system (referred to here as TAS) which creates a free photoacid upon exposure is shown to produce a low line edge roughness (LER) of 3.9 nm (3 σ), but was limited in resolution due to photoacid diffusion. A single component molecular resist with a covalently bound non-ionic photoacid generator (referred to here as NBB), i.e. one in which the photoacid anion is bound to the resist core, was found to exhibit an improved resolution of 40 nm due to reduced photoacid diffusion while maintaining a good LER and line width roughness (LWR) of 3.9 nm and 5.6 nm, respectively. Despite the small size of NBB, it was found to exhibit a glass transition temperature of 82°C. It also showed good adhesion, formed high quality films, and showed no dark erosion during development. These compounds demonstrate that it is possible to form single component molecular resists using both ionic and non-ionic photoacid generators and that such small molecule resists can provide all the basic requirements to serve as functional chemically amplified resists.

Keywords: chemically amplified photoresist, molecular resist, single molecule resist, high PAG loading, line edge roughness, single component resist, photoacid generator, bound PAG molecular resist

1. INTRODUCTION

As feature sizes shrink, there is an ever increasing concern about line edge roughness (LER) and line width roughness (LWR) in photoresists. Since LWR does not appear to scale down as pattern sizes shrink, it is rapidly becoming a significant portion of the total feature size. In order to minimize the negative impact of LWR on final transistor device performance, the LWR should be < 8-10% of the final critical dimension of the resist.¹ In attempts to reduce LWR, it was discovered that there is an intrinsic property of chemically amplified resists (CARs) that has come to be known as the “RLS tradeoff”.² The RLS tradeoff basically states that there is a tradeoff between resolution, LER, and sensitivity, such that any two of these performance parameters can be reduced but at the expense of the third parameter.³ In fact, various general equations relating this tradeoff have been reported. One popular expression of the tradeoff is⁴:

$$\text{Resolution}^3 \cdot \text{LER}^2 \cdot \text{Sensitivity} \approx \text{Resist Material Constant } Z \quad (1)$$

The resist material constant is an intrinsic property of a particular CAR resist design and formulation and can be reduced by changing aspects of the resist formulation such as type of photoacid generator and amount of base quencher. Unfortunately, it appears that modern blended polymeric CAR designs have minimized this product near its lower limits for such resist designs, but the performance of these resists still does not meet the future requirements of the ITRS roadmap⁵ and LER appears to reach a limiting value of approximately 5 nm after development.⁶

In an attempt to overcome these current limitations, new classes of CARs have been developed. The most notable new classes of materials have been molecular glass photoresists⁷⁻¹² and polymer-bound photoacid generator (PAG)

photoresists¹³⁻¹⁸. Molecular glass photoresists were originally introduced because it was thought that the reduction in resist molecule pixel size would improve LER. However, it appears that when based on traditional blended CAR designs, these molecular resists generally do not have a significant advantage in LER as compared to polymeric CAR resists and most are still limited to a minimum LER of 5 nm.¹⁹ Polymer-bound PAG resists were introduced to improve resolution by reducing the acid diffusion length of photoacids, but have also been shown to provide LER improvements with little impact on resist sensitivity.¹³

We have proposed a new class of CARs known as single component molecular glass resists or single molecule resists.²⁰⁻²¹ Single molecule resists are resists based on a single molecular species which consists of a molecular glass core compound that contains all of the functional groups required to act as a CAR including PAG functional groups, base solubilizing groups blocked by acid labile protecting groups, and typically, but not always, a sulfonic acid anion that is directly attached to the molecular glass core. Figure 1 is a diagram that demonstrates this design concept. Our view is that this single molecule design approach combines the benefits of molecular glass resists with those of polymer-bound PAGs to offer a number of significant advantages over current CAR materials that can potentially lead to improved resolution and lower LER performance, all while maintaining good resist sensitivity.

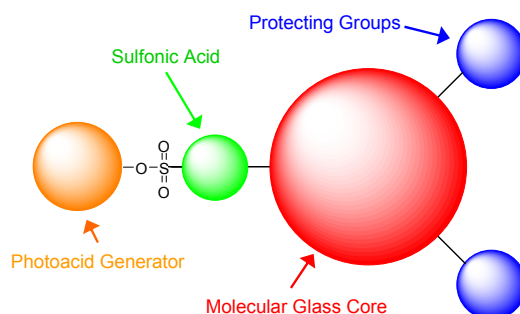


Figure 1. Schematic of the single molecule CAR design concept demonstrating the combination of all required CAR functionalities into a single small molecule.

The major advantages of single component molecular resists can be summarized using the three main benefits that they provide over other CAR systems. They provide the opportunity to ensure homogeneity of the resist film since they have no physically blended additives such as PAGs or base quencher combined with their small molecule nature which can provide for truly monodisperse resists. They also provide the ability to utilize very high PAG loadings which is beneficial because it can improve sensitivity and also appears to improve LER.²² The third advantage of this design approach is that it provides the ability to tightly control the photoacid diffusion behavior. Since the acid anion is bound to the molecular glass core, the acid diffusion coefficient can be tuned by changing the size of the core. It also should have a very uniform diffusion coefficient throughout the film, as opposed to polymer-bound PAGs which can have a distribution of diffusion coefficients due to the polydispersity of the polymer resist molecules.

To demonstrate the viability of this resist design approach, single component molecular resists utilizing the two main forms of photoacid generators, namely ionic and non-ionic PAGs, were synthesized and exercised experimentally. Figure 2 shows the structure of the compounds synthesized and investigated in this work. TAS is an ionic single molecule resist that is based on a triarylsulfonium PAG that has been functionalized with base-soluble groups that were then protected. It has been made with a variety of anions that impart different properties to the molecular resist, and these derivatives are discussed elsewhere.²³ The best positive tone performance in the series of TAS compounds investigated was obtained using TAS with a hexafluoroantimonate counter-ion and that particular TAS compound will be the derivative referred to in this paper. In this case, the TAS compounds produce a free photoacid that does not remain bound to the original large molecular resist core, but the HSBF₆ photoacid is itself large and is known to possess a relatively low diffusion coefficient in resist matrices. DPI-BocNpS is a second ionic single component molecular resist and is based on a diphenyliodonium PAG attached to a naphthalene-sulfonate core protected by tBoc. In the case of DPI-BocNpS, the sulfonic acid produced upon irradiation remains attached to the original main molecular resist core. However, NBB as shown in Figure 2 is the primary focus of this paper and is the first example of a chemically amplified

non-ionic single component molecular resist. NBB consists of a norbornene dicarboximide PAG attached to a sulisobenzene core.

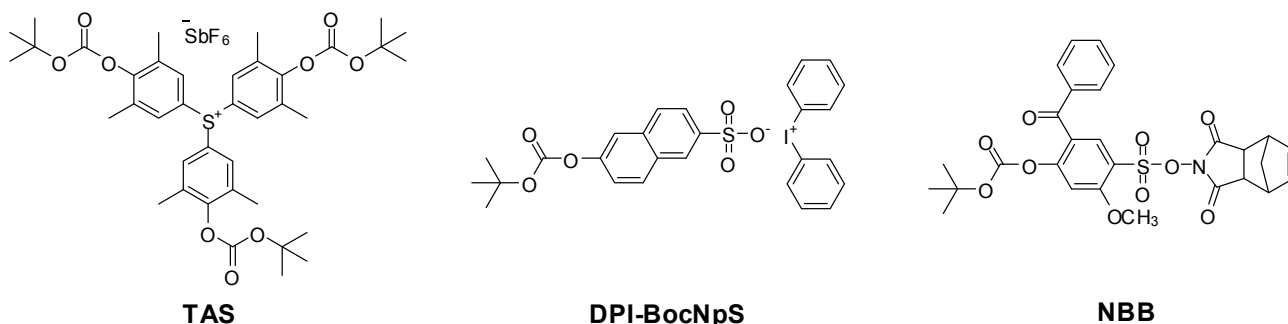


Figure 2. Chemical structures of the single component molecular resists.

2. EXPERIMENTAL

2.1 Materials and Methods

All reagents and solvents used were purchased from either Sigma-Aldrich, TCI America, or Alfa-Aesar. A Varian Mercury Vx 300 was used to collect NMR. Resist solutions were made using cyclohexanone as a casting solvent and filtered through 0.2 μm PTFE filters. All post-apply bakes were done at 90°C for 2 minutes unless otherwise noted. Film thicknesses were measured using a M-2000 spectroscopic ellipsometer (J.A. Woolam, Inc.) over the wavelengths of 350 to 1000 nm. For e-beam lithography, the resist solution was spin-coated on to a 46 nm thick silicon nitride membrane window contained in a silicon wafer support structure.²⁴ The resist film was exposed using JEOL JBX-9300FS electron-beam lithography system with 100keV acceleration voltage, 2 nA current, and 10 nm single-pixel shot pitch. The patterns produced by e-beam lithography were imaged using a LEO 1530 thermally assisted field emission SEM with 2keV acceleration voltage. The original image was off-line processed with background intensity subtraction and adaptive Gaussian-noise filtering. Critical dimension (CD) measurements, and the whole spatial-frequency $3\sigma\text{LER}$ and $3\sigma\text{LWR}$ spectra of the resist pattern were averaged from 10 different line-space patterns with a 1 μm measurement length.

2.2 Synthesis of TAS

The synthesis of TAS and its similar derivatives can be found elsewhere.²³

2.3 Synthesis of DPI-BocNpS

Diphenyliodonium 6-hydroxynaphthalene-2-sulfonate

Diphenyliodonium chloride (0.5 g, 1.58 mmol) was dissolved in 30-40 mL of deionized water. An equimolar amount of sodium 6-hydroxynaphthalenesulfonate (0.389 mg, 1.58 mmol) was dissolved in 3-5 mL of water. The naphthalene solution was slowly dripped onto the diphenyliodonium solution and a white precipitate formed. The precipitate was filtered to yield pure diphenyliodonium 6-hydroxynaphthalene-2-sulfonate. Yield = 81% $^1\text{H-NMR}$ (300 MHz, DMSO) δ (ppm) 9.79 (s, 1H), 8.25 (d, 4H), 7.97 (s, 1H), 7.77 (d, 1H), 7.64 (t, 4H), 7.57 (m, 2H), 7.50 (t, 2H), 7.07 (s, 1H), 7.00 (d, 1H).

Diphenyliodonium 6-tert-butoxycarbonyloxynaphthalene-2-sulfonate

Diphenyliodonium 6-hydroxynaphthalene-2-sulfonate (0.4 g, 0.793 mmol) was slurried in 20-30 mL of acetonitrile along with 4-dimethylaminopyridine (0.010 g, 0.0793 mmol). Boc anhydride (0.260 g, 1.19 mmol) was dissolved in 3-5 mL of acetonitrile and dripped into the reaction mixture. Upon addition of boc anhydride, the diphenyliodonium sulfonate dissolved into the acetonitrile as it was protected, giving a clear solution. After stirring overnight, a fine white precipitate appeared in the reaction flask. This precipitate was filtered to give pure diphenyliodonium 6-tert-

butoxycarbonyloxynaphthalene-2-sulfonate. Yield = 85.7% ¹H-NMR (300 MHz, DMSO) δ (ppm) 8.23 (d, 4H), 8.15 (s, 1H), 8.02 (d, 1H), 7.85 (d, 1H), 7.72 (m, 1H), 7.70 (d, 1H), 7.64 (t, 2H), 7.50 (t, 4H), 7.36 (d, 1H), 1.52 (s, 9H),

2.4 Synthesis of NBB

The synthetic scheme used to synthesize NBB is shown in Figure 3 below.

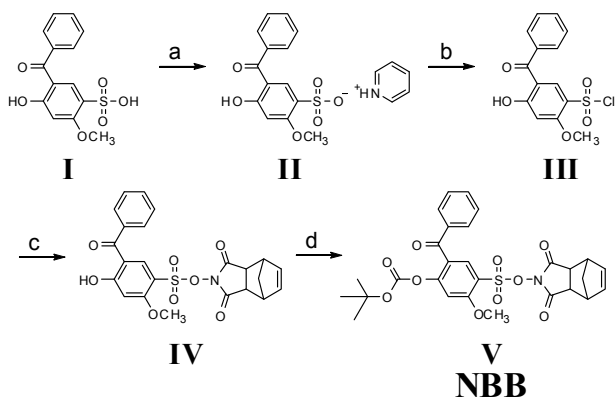


Figure 3. Synthetic strategy of NBB: (a) pyridine, THF; (b) SOCl₂, DMF; (c) NDI-OH, pyridine, THF; (d) Boc₂O, DMAP, THF.

Pyridinium 5-benzoyl-4-hydroxy-2-methoxybenzenesulfonate (II)

II and III were synthesized analogously to the procedure in reference 25. 5-benzoyl-4-hydroxy-2-methoxybenzenesulfonic acid (8.00 g, 25.94 mmol) was dissolved in 80 mL of warm tetrahydrofuran (THF). As pyridine (3.078 g, 38.92 mmol) was slowly dripped into the solution, a fine white precipitate formed. After stirring for 30 minutes, it was poured onto 125 mL pentane, stirred for another 15 minutes, filtered, and dried *in vacuo* to give II. Yield = 94% ¹H-NMR (300 MHz, DMSO) δ (ppm) 8.91 (d, 2H), 8.57 (t, 1H), 8.05 (t, 2H), 7.91 (s, 1H), 7.7-7.5 (m, 5H), 6.57 (s, 1H), 3.78 (s, 3H).

5-Benzoyl-4-hydroxy-2-methoxybenzenesulfonyl chloride (III)

II (6.00 g, 15.49 mmol) was slowly added over 15 minutes to a solution of thionyl chloride (7.368 g, 61.93 mmol) and 3 drops of dimethyl formamide. After addition, the mixture was stirred for 2-3 hours at 65°C. The mixture was cooled and added drop-wise to 60 mL of ice water. A pale orange solid was filtered and dissolved in 80 mL of chloroform. The chloroform solution was washed twice with 50 mL of dilute HCl solution, and 50 mL of deionized water. The organic layer was dried over MgSO₄, and the solvent was removed by rotary evaporator to give III as a solid. Yield = 72% ¹H-NMR (300 MHz, CDCl₃) δ (ppm) 8.32 (s, 1H), 7.66-7.55 (m, 5H), 6.68 (s, 1H), 4.12 (s, 3H).

5-Norbornene-2,3-dicarboximidyl 5-benzoyl-4-hydroxy-2-methoxybenzenesulfonate (IV)

III (3.00 g, 9.18 mmol) and NDI-OH (1.809 g, 10.10 mmol) were dissolved in 40 mL of tetrahydrofuran and cooled on an ice bath. Pyridine (1.089 g, 13.77 mmol) in 5 mL of THF was slowly dripped into the cooled THF solution. After complete addition of pyridine, the solution was allowed to warm to room temperature and a white precipitate began to form. After stirring overnight, 20 mL of dichloromethane and 20 mL of deionized water were added to the reaction flask and stirred until all solids had dissolved. The organic layer was separated and washed twice with 20 mL of saturated NaHCO₃ solution, 20 mL of saturated NaCl solution, 20 mL of deionized water, dried over MgSO₄, and concentrated by rotary evaporator. The residue was dissolved in a minimal amount of THF and dripped into deionized water to give IV as a solid. Yield = 45% ¹H-NMR (300 MHz, CDCl₃) δ (ppm) 8.14 (s, 1H), 7.65-7.5 (m, 5H), 6.64 (s, 1H), 5.97 (s, 2H, CH=CH), 4.06 (s, 3H, OCH₃), 3.37 (s, 2H), 3.19 (s, 2H), 1.70 (d, 1H), 1.46 (d, 1H).

5-Norbornene-2,3-dicarboximidyl 5-benzoyl-4-tert-butoxycarbonyloxy-2-methoxybenzenesulfonate (V, NBB)

IV (1.00 g, 2.13 mmol) and 4-dimethylaminopyridine (0.0129 g, 0.106 mmol) were dissolved in 20 mL of tetrahydrofuran (THF). Di-tert-butyl dicarbonate (0.697 g, 3.19 mmol) dissolved in 5 mL of THF was added to the

reaction mixture and stirred overnight at room temperature. Dichloromethane (10 mL) and 10 mL of deionized water were added to the reaction mixture. The organic layer was separated and washed with 15 mL of saturated NaCl solution, twice with 15 mL of deionized water, dried over MgSO_4 , and concentrated by rotary evaporator. Hexane was added to the residue and the white precipitate filtered to give **V**. Yield = 54% $^1\text{H-NMR}$ (300 MHz, CDCl_3) δ (ppm) 8.02 (s, 1H), 7.73-7.46 (m, 5H), 6.98 (s, 1H), 6.10 (s, 2H, CH=CH), 4.09 (s, 3H, OCH_3), 3.39 (s, 2H), 3.20 (s, 2H), 1.72 (d, 1H), 1.43 (d, 1H), 1.39 (s, 9H, tBu).

3. RESULTS AND DISCUSSION

3.1 TAS

Full details about EUV and e-beam imaging performance and properties of TAS can be found elsewhere.²³ A short summary of performance under 100 keV e-beam is given below for comparison with NBB. Several derivatives of TAS were made with different anions other than SbF_6^- , but they all suffered from significant enough dark loss that reasonable positive tone imaging was limited due to the intrinsic solubility of the ionic compounds in water.

High resolution imaging of TAS-tBoc-SbF₆ was first carried out using 100 keV e-beam lithography with a PEB of 75°C. Under these conditions, the sensitivity was found to be 190 $\mu\text{C}/\text{cm}^2$ and the contrast was 2.1. High resolution patterning resulted in approximately 100 nm 1:1 lines/spaces, but smaller pitches were limited due to photoacid diffusion. Figure 4 shows 55 nm lines and 105 nm spaces that were nominally printed at 80 nm 1:1 lines/spaces, but line slimming due to photoacid diffusion reduced the lines to 55 nm. Smaller patterns suffered from severe pattern collapse as the aspect ratio was greater than 2.5:1. From these imaging results, the LER (3σ) was found to be 3.9 nm. While this single component resist shows a relatively low LER, it still suffers from resolution limitation due to diffusion of a small, free photoacid.

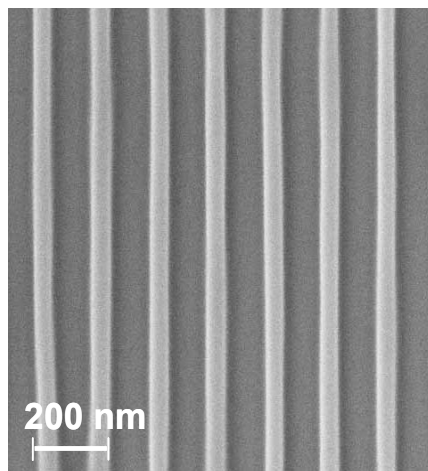


Figure 4. E-beam (100 keV) imaging results for TAS (75°C PEB) demonstrating a LER of 3.9 nm for 55 nm lines and 105 nm spaces.

3.2 DPI-BocNpS

While TAS showed improvements in LER, it was still resolution limited due to acid diffusion. To improve upon the resolution limitations of TAS, an iodonium based single component molecular resist was synthesized with a much larger photoacid. An iodonium PAG was chosen instead of a triarylsulfonium type PAG to compare the differences in sensitivity of the two PAGs at this high loading. DPI-BocNpS was synthesized with good purity in a simple two-step procedure. After it was synthesized, DPI-BocNpS had poor solubility in most common casting solvents such as cyclohexanone and PGMEA, but good films could be cast out of DMF. While the film quality was good, the entire film very rapidly dissolved in aqueous base and pure water. This was similar to what was observed in most of the TAS derivatives, and is likely a significant hurdle to the implementation of onium salt PAG based single component molecular resists. When the film is exposed to DUV light and given a PEB of 90°C, it shows thickness loss indicative of

tBoc group deprotection. This indicates that the material is making photoacid and deprotection of the tBoc groups can be achieved, but the dissolution rate difference between the unexposed and exposed areas (the dissolution rate contrast) is not significant enough to enable the patterning of this material.

3.3 NBB

Due to the significant solubility problems encountered with the ionic PAG based single component systems, a non-ionic PAG based single component molecular resist (NBB) was synthesized. Figure 3 outlines the general synthetic strategy for NBB. Due to the steric hindrance of the hydroxyl group of I, no protection was required before conversion to the sulfonyl chloride. However, formation of the pyridinium salt before conversion to the sulfonyl chloride improved overall yield of the sulfonyl chloride. Coupling of III to NDI-OH could be carried out without protection of the hydroxyl group on III because pyridine was used as the base. It was previously found that for a similar 4-hydroxybenzenesulfonyl chloride, self-condensation would not occur using pyridine but would occur when using stronger bases such as triethylamine.²⁶

NBB formed excellent films by spin-casting from cyclohexanone solution and showed no signs of crystallization, even after several weeks elapsed after casting films of the material. The adhesion to silicon was good, both with and without hexamethyldisilazane (HMDS) priming of the substrate. No measureable dark erosion of NBB occurred over 30-60 seconds of immersion in 0.261N TMAH. This is expected due to the fully protected, non-ionic nature of the compound. Photoacid generation in NBB was confirmed by loading it into another molecular glass resist (THPE-THP)²⁷ at 10 weight percent and exposing films of the mixture to 248 nm ultraviolet light.

Since most patterning requirements for this material will require sub-150 nm film thicknesses, it is more useful to determine the glass transition temperature of the ultrathin film rather than that of the bulk sample.²⁸ The glass transition temperature (T_g) of NBB was determined by spin-coating a film onto a native oxide covered silicon wafer and measuring the film thickness as a function of temperature. The discontinuity in the thickness versus temperature curve corresponds to the material's glass transition temperature and is indicative of the change in coefficient of thermal expansion in the materials as it transitions from its glass to melt states. Figure 5 shows the first and second heating curves for a thin NBB film. Using this method, the T_g of NBB was determined to be 82°C. While this may not be considered an extremely high T_g for a resist, it is quite high for such a small molecular glass with a modest molecular weight of only 569.58 g/mol. For comparison, this T_g is nearly the same as another reported fully tBoc protected molecular glass resist whose molecular weight was 1315.5, and is higher than another fully tBoc protected molecular resist reported in the same paper whose molecular weight was 903.1.²⁹ As expected, structural effects have a large effect on T_g in these small molecule materials.

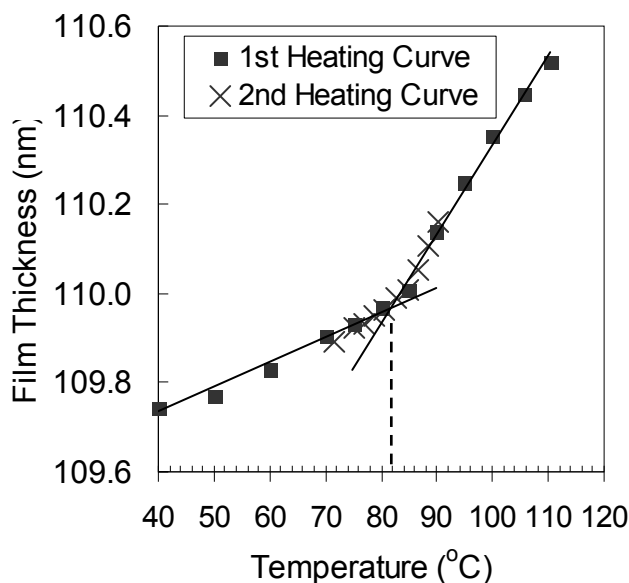


Figure 5. Thickness vs. temperature heating curve for NBB using ellipsometer with hot stage.

High energy (100 keV) e-beam lithography was used to investigate the suitability of NBB as a high resolution material before EUV patterning was performed. Figure 6 shows the e-beam contrast curve for NBB with a 90°C PEB for 1 minute. Lower PEB temperatures were unsuitable because the dose-to-clear increased by more than a factor of three. The sensitivity (dose-to-clear) was 670 $\mu\text{C}/\text{cm}^2$, and the contrast ratio was 5.8. This is a reasonable contrast value, but the dose-to-clear is quite high, nearly 3 times that of TAS. One reason is that photolysis of this PAG liberates an aryl sulfonic acid, which is a strong acid, but not as strong as the superacids commonly used in photoresists such as perfluorobutanesulfonate or hexafluoroantimonate. The sulfonic acid made by NBB does not efficiently carry out deprotection below 90°C, and it is likely that even 90°C is not the optimal PEB temperature for this system. Unfortunately, higher temperatures lead to higher levels of acid diffusion and pattern blur. Another possible problem with this compound's sensitivity is that the PAG used is 5-norbornene-2,3-dicarboximide, and dicarboximide PAGs have consistently shown lower photoreaction rate constants than the commonly used onium salt PAGs. Some studies also indicate that this type of PAG requires a stoichiometric amount of water for every acid generated. Since these very thin films are exposed in the high vacuum of the e-beam chamber, there is likely very little adventitious water in the resist which could lead to inefficient acid production. While the sensitivity of NBB is not as high as one would like, the sensitivity is as one might expect comparing NBB to TAS and is sufficient for imaging of the material.

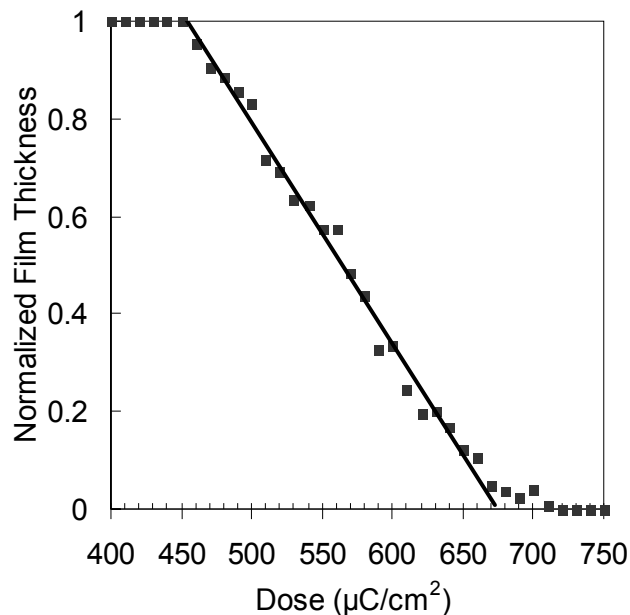


Figure 6. Contrast curve for NBB under e-beam (100 keV) for 90°C PEB.

High resolution e-beam (100 keV) imaging of NBB is seen in Figure 7 for a 90°C PEB. The linewidth along with the line/space pattern is shown on the image. The 80 nm lines are shown at a higher resolution to better demonstrate the pattern fidelity. The resist showed good line/space patterns down to 70 nm lines, and smaller half-pitch patterns resolved but suffered from pattern collapse as the aspect ratio of began to exceed roughly 2:1. Lines were resolved down to 40 nm for 1:3 line/spaces, implying that at least 40 nm half-pitch could be obtainable in this system using thinner resist films or modified development and rinse procedures.

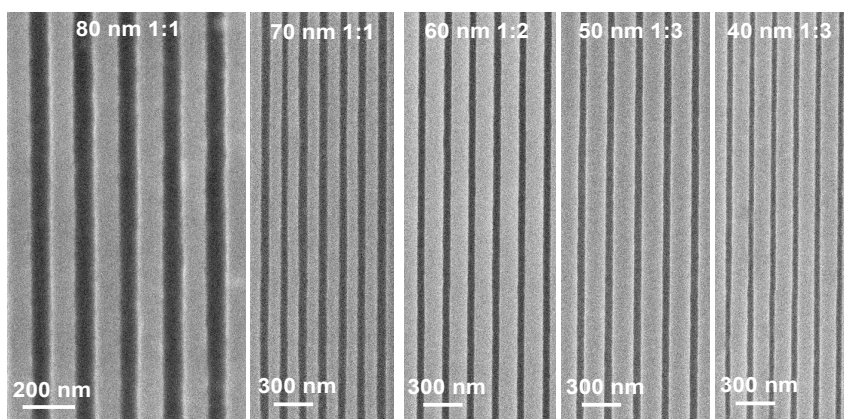


Figure 7. High resolution SEM pictures of line-space patterns achieved in NBB using 100 keV e-beam patterning.

NBB was able to resolve 40 nm lines with no base quencher added, even though its PEB was above its T_g . The improved resolution of this system relative to TAS is likely due to the fact that the photoacid was integrated into the molecular glass core, reducing the effective acid diffusion length. Although the molecular glass core was rather small, it still provided enough of a decrease in diffusion coefficient to improve performance. By moving to larger cores in the future, the resolution could likely be improved even more.

The line edge roughness of resists has become an increasingly important issue as feature sizes decrease. The LER and LWR for NBB was determined using the 80 nm 1:1 line/space patterns as seen in Figure 7. The LER (3σ) was 3.9 nm and LWR (3σ) was 5.6 nm for an inspection length of 1000 nm. Although these values are still not small enough to meet ITRS patterning targets for upcoming IC nodes, they are a significant improvement compared to most current resists which show LER values of 5 nm and larger.⁶ The single component molecular resist approach appears to have provided a potential improvement in LER as compared to traditional low-PAG loading blended resists. Improvement of the dicarboximide PAG and use of a larger molecular glass cores would likely allow for even lower LER in future single component molecular resists.

4. CONCLUSIONS

A series of single component molecular resists were designed, synthesized, characterized, and patterned using 100 keV e-beam lithography. TAS, an onium salt based single molecule resist, printed 50 nm lines with a low LER of 3.9 nm. DPI-BocNpS was designed with a more bulky sulfonic acid moiety, but suffered from severe water solubility that prevented it from being patterned. NBB, a single component molecular resist with a covalently bound non-ionic photoacid generator, was found to exhibit 40 nm resolution with low LER and LWR (3.9 nm and 5.6 nm) along with a glass transition temperature of 82°C. It also showed good adhesion, formed high quality films, and showed no dark erosion during development. A few structural problems in this compound likely negatively impacted the sensitivity of the material ($670 \mu\text{C}/\text{cm}^2$ at 100 keV), but these issues can all be improved in future designs. NBB demonstrates that a small molecule single component resist can be made using non-ionic PAGs and this compound shows some of the promise that this class of materials holds for high resolution, low LER materials with good sensitivity.

ACKNOWLEDGEMENTS

The authors would like to gratefully acknowledge Intel Corporation for funding this research and would also like to thank Dr. Jeanette Roberts, Dr. Steve Putna, Dr. Todd Younkin, and Dr. Wang Yueh at Intel for helpful discussions related to this work. AZ Electronic Materials and Dr. Ralph Dammel are also gratefully acknowledged for the generous donation of the developers used in this work.

REFERENCES

1. M. Chandhok, Proc. SPIE **6519**, 6519A (2007).
2. R. L. Bristol, Proc. SPIE **6519**, 65190W (2007).
3. G.M. Gallatin, Proc. SPIE **5754**, 38 (2005).
4. T. Wallow, C. Higgins, R. Brainard et al., Proc. SPIE, **6921**, 69211F (2008).
5. ITRS, International Technology Roadmap for Semiconductors, Lithography, <http://public.itrs.net/>, 2007.
6. A.R. Pawlowski, A. Acheta, I. Lalovic, B. La Fontaine, H. Levinson, Proc. SPIE **5376**, 414 (2004).
7. D. Yang, S.W. Chang, C.K. Ober, J. Mater. Chem. **16**, 1693 (2006).
8. J. Y. Dai, S.W. Chang, A. Hamad, D. Yang, N. Felix, C.K. Ober, Chem. Mater. **18**, 3404 (2006).
9. T. Hirayama, D. Shiono, J. Onodera et al., Polym. Adv. Technol., **17**, 116, (2006).
10. T. Hirayama, D. Shiono, H. Hada et al., J. Photopolym. Sci. Technol., **17**, 435 (2004).
11. A. De Silva, N. M. Felix, and C. K. Ober, Adv. Mater., **20**, 3355, (2008).
12. K. Kojima, T. Hattori, H. Fukuda et al., J. Photopolym. Sci. Technol., **19**, 373 (2006).
13. C. T. Lee, C. L. Henderson, M. X. Wang et al., J. Vac. Sci. Technol. B. **25**, 2136 (2007).
14. M. X. Wang, C.T. Lee, C. L. Henderson, et al., Proc. SPIE **6519**, 65191F (2007).
15. M. X. Wang, K. E. Gonsalves, M. Rabinovich et al., J. Mater. Chem., **17**, 1699, (2007).
16. K. E. Gonsalves, M. Thiyagarajan, and K. Dean, J. Micro/Nanolithography, Microfab. Microsys., **4**, 029701, (2005).
17. M. X. Wang, W. Yueh, and K. E. Gonsalves, J. Fluorine Chem., **129**, 607 (2008).
18. C. T. Lee, C. L. Henderson, M. X. Wang et al., Microelectron. Eng., **85**, 963, (2008).
19. A. De Silva, N. Felix, J. Sha, J.K. Lee, C.K. Ober, Proc. SPIE **6923**, 69231L, (2008).
20. R. A. Lawson, C.T. Lee, R. Whetsell, et al., Proc. SPIE **6519**, 65191N (2007).
21. R. A. Lawson, C.T. Lee, W. Yueh, et al., Proc. SPIE **6923**, 69230K, (2008).
22. R. A. Lawson, C.T. Lee, W. Yueh, et al., Proc. SPIE **6923**, 69230Q, (2008).
23. R. A. Lawson, C.T. Lee, L. M. Tolbert, and C.L. Henderson, Microelectron. Eng., doi:10.1016/j.mee.2008.11.043 (2009).
24. A. W. Grant, Q.H. Hu, B. Kasemo, Nanotechnology, **15**, 1175, (2004).
25. T. N. Myers, U.S. Patent 5041545, (1991).
26. R.W. Campbell, H.W. Hill Jr, Macromolecules **6**, 492 (1973).
27. R. A. Lawson, C.T. Lee, R. Whetsell, W. Yueh, L. Tolbert, and C. L. Henderson, J. Vac. Sci. Technol. B. **25**, 2140 (2007).
28. L. Singh, P. J. Ludovice, and C. L. Henderson, Thin Solid Films, **449**, 231 (2004).
29. A. De Silva, J.K. Lee, X. Andre, N. Felix, H.B. Cao, H. Deng, C.K. Ober, Chem. Mater. **20**, 1606 (2008).